capillaries.[1] Since the reticuloendothelial systems of the liver and spleen also extract smaller colloids, some of the uptake exhibited by these two organs may be due to colloid formation in the blood. However, the moderate spleen uptake suggests that this is not responsible for the substantial localization of these compounds in the liver.

Even though the complexes are neutral, they did not efficiently cross the blood–brain barrier (although the presence of ethanol may have affected this) and so would need substantial modification to be developed as candidates for brain-imaging agents. On the other hand, the heart uptake exhibited by I was unexpected and derivatives that would cause this uptake to be accumulative might prove useful. Since these compounds are presently efficiently prepared only with millimolar concentrations of technetium, they cannot now be easily derived from the no-carrier-added ^{99m}Tc solutions normally used in radiopharmaceutical synthesis, which are typically in the nano- to micromolar range. Nevertheless, a better understanding of the mechanism of formation of these complexes may yield reactions capable of synthesizing these types of complexes at low technetium concentration.

Conclusion. These complexes are unusual examples of unsymmetrical, mixed-valent complexes in which the unpaired electron is delocalized[22] and in which strong tetragonal distortion is evident in the IVCT bands. The high solubility of these complexes in low dielectric solvents, their adherence to Beer's law, their small solution conductivities, their failure to be immediately retained by ion exchange columns, and clear evidence for binuclear species in the solution EPR spectra provide convincing evidence that these compounds are essentially identical in both solution and the solid state. The presence of only monodentate ligands and the ability to undergo electron transfer suggest these complexes as a synthetic route to lower technetium oxidation states. This is especially attractive since the main obstacle to obtaining these species—elimination of multiply bonded oxygen—has been overcome. Finally, the ability to easily prepare both asymmetric and dissymmetric technetium complexes with heterocyclic ligands opens synthetic avenues for the preparation of technetium complexes which can bind to biologically important molecules such as nucleotides, coenzymes, and nucleic acids. Indeed, their tendency to slowly and irreversibly bind to ion exchange materials suggests that they may be able to firmly attach to charged biopolymers, such as nucleic acids.

Acknowledgment. This work was supported by PHS Grant GM26390. ESR spectra and helpful discussions on their interpretation were provided by Drs. Hans Van Willigen and T. K. Chakesandra at the University of Massachusetts (Boston). Dr. Jack Spence of Utah State University generously provided the VAX version of EPROW and Dr. Dennis Chasteen of the University of New Hampshire guided us in its use. We are also grateful to Prof. Harvey Shugar at Rutgers University for collecting the crystallographic data set.

Registry No. I, 112816-10-1; II, 112816-18-9; III, 112816-15-6; $[Cl(Pyr)_4TcOTcCl_4(Pyr)]$, 112816-08-7; $[Br(Pyr)_4TcOTcBr_4(Pyr)]$, 112816-09-8; $[Br(Pic)_4Tc{\cdot}OTcBr_4(Pic)]$, 112816-11-2; $[Cl(Lut)_4TcOTcCl_4(Lut)]$, 112816-12-3; $[Cl(Pyr)_3ClTcOTc(Pyr)Cl_3(Pyr)]$, 112816-13-4; $[Br(Pyr)_3BrTcOTc(Pyr)Br_3(Pyr)]$, 112816-14-5; $[Br(Pic)_3BrTcOTc(Pic)Br_3(Pic)]$, 112816-16-7; $[Cl(Lut)_3ClTcOTc(Lut)Cl_3(Lut)]$, 112816-17-8; $[(n\text{-}Bu)_4N][TcOCl_4]$, 92622-25-8; $[(n\text{-}Bu)_4N][TcOBr_4]$, 92622-23-6; $[(n\text{-}Bu)_4][TcCl_6]$, 112816-19-0; $[(n\text{-}Bu)_4N][TcBr_6]$, 112816-20-3; $(NH_4)TcO_4$, 34035-97-7; $[(n\text{-}C_4H_9)_4N][TcO_4]$, 111127-64-1.

Supplementary Material Available: Tables of temperature factors for non-hydrogen atoms, bond distances and angles for picoline ligands, electronic spectra for $[Cl(Pic)_4Tc\text{–}O\text{–}TcCl_4(Pic)]$ in various solvents, complete listings of infrared, figures showing closest contacts of picoline rings in I, solid state and room temperature EPR spectra, and figures of UV–visible spectra and biological tissue distributions (24 pages); listing of calculated and observed structure factor amplitudes for $[(Pic)Cl_3(Pic)Tc\text{–}O\text{–}TcCl(Pic)_3Cl]$ and $[Cl(Pic)_4Tc\text{–}O\text{–}TcCl_4(Pic)]$ (64 pages). Ordering information given on any current masthead page.

Cobalt and Manganese Complexes of a Schiff Base Biquinone Radical Ligand

Scott K. Larsen and Cortlandt G. Pierpont*

Contribution from the Department of Chemistry and Biochemistry, University of Colorado, Boulder, Colorado 80309. *Received July 7, 1987*

Abstract: Reactions between 3,5-di-*tert*-butylcatechol, aqueous ammonia, and divalent metal ions produce neutral complexes containing a tridentate ligand formed by the Schiff base condensation of two catechol molecules with NH_3. The free ligand may exist in electronic forms ranging in charge from +1 to −3, and, in complexes formed with divalent metal ions that are not electroactive, the ligand bonds in the −1 form, $M^{II}(Cat\text{-}N\text{-}BQ)_2$. With electroactive metal ions a charge balance is reached between metal and ligands by intramolecular electron transfer. The complex prepared with Mn(II) shows structural features that are consistent with a complex containing Mn(IV) with ligands in the radical dianion Cat-N-SQ form, $Mn^{IV}(Cat\text{-}N\text{-}SQ)_2$. The complex contains one unpaired electron due to coupling between the two radical ligands and the d^3 metal ion. Isotropic and anisotropic EPR spectra verify that the unpaired electron resides in a metal-localized orbital. Electrochemistry shows redox activity for both metal and ligands and the electronic spectrum of the complex shows four intense bands in the near-infrared. The related complex prepared with Co(II) shows structural features of Co(III), requiring one ligand in the −1 form and the second in the form of the −2 radical, $Co^{III}(Cat\text{-}N\text{-}BQ)(Cat\text{-}N\text{-}SQ)$. This molecule also contains a single unpaired electron, but with the diamagnetic metal ion, the electron is in a ligand-localized orbital. The EPR spectrum verifies this, but shows an unusually simple hyperfine pattern consisting of 16 lines due to coupling to the $I = {}^7/_2$ metal and one $I = {}^1/_2$ center, presumably one ligand proton. This result appears to indicate that the unpaired electron is regionally localized on one ligand on the EPR time scale.

Studies on the coordination of semiquinonate and catecholate ligands to transition-metal ions have shown that the intramolecular charge distribution between metal and quinone is sensitive to several effects. The increase in orbital energy on the metal for third-row metals relative to metals of the first transition series results in catecholate complexes of hexavalent metal ions, M^{VI}-

0002-7863/88/1510-1827$01.50/0

$(Cat)_3$ for W, Re, and Os,[1-3] while Cr, Mn, and Fe analogues contain di- and trivalent metals bonded to semiquinonate ligands in $M^{II}(SQ)_2$ and $M^{III}(SQ)_3$ complexes.[4-6] The effect of counter-ligand donation on metal orbital energy and metal–quinone charge distribution is apparent in copper complexes where, with hard nitrogen donor ligands, the quinone is the reduced center in $(N-N)Cu^{II}(Cat)$, relative to the phosphine complexes $(P-P)Cu^{I}(SQ)$ where the metal is in the reduced form.[7] More subtle effects contribute to the sensitivity to overall complex charge found for the neutral and anionic vanadium complexes $V^{III}(SQ)_3$ and $V^{V}(Cat)_3^-$,[8] and to the thermal sensitivity of the Co and Mn complexes containing nitrogen-donor counter ligands (eq 1). The

$$Co^{II}(bpy)(DBSQ)_2 \rightleftarrows Co^{III}(bpy)(DBSQ)(DBCat)$$
$$Mn^{II}(py)_2(DBSQ)_2 \rightleftarrows Mn^{IV}(py)_2(DBCat)_2 \quad (1)$$

tetrameric complexes formed by treating cobalt or manganese carbonyl with 3,5-di-*tert*-butyl-1,2-benzoquinone dissociate to form monomeric adducts when treated with nitrogen-donor ligands.[5,9] In toluene solution over the temperature range −40 to 40 °C both complexes show thermochromic and magnetic changes that are consistent with equilibria involving species related by transfer of one or two electrons between metal and the quinone ligands. Extension of this work to include complexes prepared with the ammine ligand has resulted in a series of new compounds containing a tridentate biquinone ligand formed by Schiff base condensation of two 3,5-di-*tert*-butylsemiquinone molecules.

Girgis and Balch found that by treating a solution containing 3,5-di-*tert*-butylcatechol and a divalent metal ion with aqueous ammonia in the presence of air, complexes of the 3,5-di-*tert*-butyl-1,2-quinone 1-(2-hydroxy-3,5-di-t-butylphenyl)imine (Cat-N-BQ) anion could be formed (eq 2).[10] In principle, this ligand

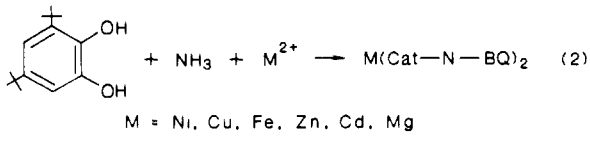

may exist in forms ranging in charge from +1 to −3. Air oxidation

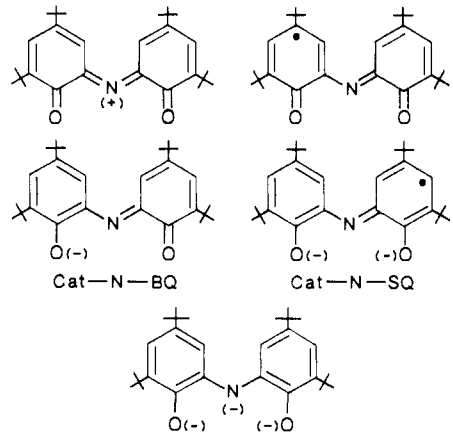

of the uncomplexed Cat-N-BQ anion results in formation of the neutral, paramagnetic SQ-N-BQ radical[11] and reduction of the monoanion leads to the Cat-N-SQ radical dianion.[12] All four neutral and anionic electronic forms of the ligand may potentially contribute to its coordination properties with metal ions. With the large number of accessible redox states for the ligand and the additional electrochemical activity of the complexed metal ion, bis complexes of this ligand system may show exceptional electrochemical properties. As with the complexes of simple quinone ligands, additional questions arise concerning the charge distribution between metal and ligand in cases where both exhibit redox chemistry. In this report we describe the products obtained when reaction 2 is carried out with the divalent metals Co^{2+} and Mn^{2+} and describe experiments carried out to investigate their redox properties and charge distribution.

Experimental Section

Synthetic Procedures. $Co(C_{28}H_{40}NO_2)_2$. A solution of 3,5-di-*tert*-butylcatechol (0.53 g, 2.41 mmol) in 30 mL of 95% ethanol was added to a solution of $CoCl_2 \cdot 2H_2O$ (0.10 g, 0.58 mmol) in 5 mL of water. Initially upon addition of 2.5 mL of concentrated aqueous ammonia the solution turned dark olive green. After 30 min of stirring the solution had become dark red-purple and a precipitate of the complex had formed. After 4 h of stirring the solution was filtered and the purple complex was washed with aqueous ethanol and vacuum dried. Yield: 0.38 g, 72%. Crystals of the complex suitable for crystallographic analysis were grown by slow evaporation of a toluene solution.

$Mn(C_{28}H_{40}NO_2)_2$. The dark green Mn complex was synthesized by using the procedure above, by substituting $MnCl_2 \cdot 4H_2O$ for the metal salt. The complex was obtained in 75% yield. Crystals suitable for X-ray analysis were grown from toluene solution.

Physical Methods. Infrared spectra were recorded on a Beckman IR 4250 spectrometer and on an IBM IR/30 series FTIR spectrometer with samples prepared as KBr pellets. UV–vis–near-IR spectra were recorded on a Hewlett Packard 8451A diode array spectrophotometer and on a Cary 17 spectrophotometer. Magnetic susceptibility measurements were made by the Faraday technique on a Sartorius 4433 microbalance, and electron paramagnetic resonance spectra were obtained on a Varian E-109 spectrometer with DPPH used as the *g* value standard. Cyclic voltammograms were obtained with a BAS-100 electrochemical analyzer. A platinum disk working electrode and a platinum wire counter electrode were used. A Ag/Ag^+ reference electrode was used consisting of a silver acetate solution in contact with a silver wire placed in glass tubing with a Vycor frit at one end to allow ion transport. Tetra-*n*-butylammonium hexafluorophosphate was used as the supporting electrolyte, and the ferrocenium/ferrocene couple (+0.16 V vs SCE) was used as an internal standard.

Crystallographic Structure Determinations on $Co(C_{28}H_{40}NO_2)_2$ and $Mn(C_{28}H_{40}NO_2)_2$. Crystals of both complexes were mounted on glass fibers and aligned on a Nicolet P3F automated diffractometer. Photographs taken on both crystals indicated triclinic symmetry and further indicated that the two complex molecules were approximately isostructural. Unit cell dimensions are given in Table I with details of procedures used for data collection and structure determination.

Both structures were solved with direct methods and refined to the values indicated in the table. In both structure determinations one *tert*-butyl group was found to suffer from twofold rotational disorder. Methyl carbon atoms of these groups, C40, C41, and C42, were refined with isotropic thermal parameters. For both structure determinations the maximum residual electron density was found to be in the region of the disordered carbon atoms, $0.75e^-/Å^3$(Co) and $0.79e^-/Å^3$(Mn). Final positional and isotropic thermal parameters for the two structure determinations are given in Tables II and III. Tables containing anisotropic thermal parameters and structure factors for both structure determinations are available as supplementary material.

Experimental Results

When reaction 2 is carried out in the presence of Mn^{2+} and Co^{2+} samples of complexes containing the Schiff base biquinone ligand are obtained as dark green (Mn) and dark purple (Co) crystalline solids. Complexes of both metals have been characterized with crystallographic and spectroscopic methods.

Crystallographic Structure Determination on Co(Cat-N-BQ)(Cat-N-SQ). The results of our crystallographic study on the

(1) (a) Pierpont, C. G.; Downs, H. H.; Rukavina, T. G. *J. Am. Chem. Soc.* **1974**, *96*, 5573. (b) Beshouri, S. M.; Rothwell, I. P. *Inorg. Chem.* **1986**, *25*, 1962.
(2) (a) deLearie, L. A.; Pierpont, C. G. *J. Am. Chem. Soc.* **1986**, *108*, 6393. (b) deLearie, L. A.; Haltiwanger, R. C.; Pierpont, C. G. *Inorg. Chem.* **1987**, *26*, 817.
(3) Nielson, A. J.; Griffith, W. P. *J. Chem. Soc., Dalton Trans.* **1978**, 1501.
(4) Buchanan, R. M.; Kessel, S. L.; Downs, H. H.; Pierpont, C. G.; Hendrickson, D. N. *J. Am. Chem. Soc.* **1978**, *100*, 7894.
(5) Lynch, M. W.; Hendrickson, D. N.; Fitzgerald, B. J.; Pierpont, C. G. *J. Am. Chem. Soc.* **1984**, *106*, 2041.
(6) Boone, S. R.; Purser, G. H.; Pierpont, C. G.; Chang, H.-R.; Lowery, M. D.; Hendrickson, D. N, submitted for publication.
(7) Buchanan, R. M.; Wilson-Blumenberg, C.; Trapp, C.; Larsen, S. K.; Greene, D. L.; Pierpont, C. G. *Inorg. Chem.* **1986**, *25*, 3070.
(8) Cass, M. E.; Gordon, N. R.; Pierpont, C. G. *Inorg. Chem.* **1986**, *25*, 3962.
(9) Buchanan, R. M.; Pierpont, C. G. *J. Am. Chem. Soc.* **1980**, *102*, 4951.
(10) Girgis, A. Y.; Balch, A. L. *Inorg. Chem.* **1975**, *14*, 2724.
(11) Ivakhnenko, E. P. *Zh. Org. Khim.* **1983**, *19*, 886.
(12) Stegmann, H. B.; Scheffler, K. *Chem. Ber.* **1968**, *101*, 262.

Table I. Crystallographic Information on $Co(C_{28}H_{40}NO_2)_2$ and $Mn(C_{28}H_{40}NO_2)_2$

	$Co(C_{28}H_{40}NO_2)_2$	$Mn(C_{28}H_{40}NO_2)_2$
formula	$CoC_{56}H_{80}N_2O_4$	$MnC_{56}H_{80}N_2O_4$
mol wt	904.19	900.20
space group[a]	$P\bar{1}$	$P\bar{1}$
crystal system	triclinic	triclinic
a (Å)[b]	11.334 (2)	11.407 (2)
b (Å)	12.461 (2)	12.391 (3)
c (Å)	20.766 (5)	20.789 (5)
α (deg)	90.76 (2)	90.27 (2)
β (deg)	104.46 (2)	104.90 (2)
γ (deg)	104.12 (2)	104.03 (2)
volume (Å^3)	2745 (1)	2748 (1)
d_{exptl} (g/cm^3)[c]	1.07 (2)	1.07 (2)
Z	2	2
d_{calcd} (g/cm^3)	1.09	1.09
$F(000)$	978	974
crystal dimnsns (mm)	0.21 × 0.13 × 0.07	0.27 × 0.24 × 0.04
μ (cm^{-1})	3.51	2.70
no. of unique reflcns	7288	7233
no. of obsd reflcns	3574	3411
R and wR^d (obsd data)	0.0551, 0.0702	0.0608, 0.0731
no. of parameters	565	565
ratio of observations to parameters	6.3	6.0
GOF	1.164	1.460
diffractometer	Nicolet P3F	
radiation (Å)	Mo Kα (0.71069)	
temp (K)	294–297	
scan technique	θ–2θ	
2θ, min – max (deg)	3.0, 45.0	
data collected	$h,\pm k,\pm l$	
scan speed (deg/min)	2.0, 30.0	
scan range	1.0 below Kα_1 and 1.0 above Kα_2	
background	stationary crystal–stationary counter background time = 0.5 scan time	
programs	SHELXTL[e]	
scattering factors	neutral atoms[f]	
criterion	$F > 6\sigma(F)$	
weight	$1.0/(\sigma^2(F) + 0.0010F^2)$	

[a] *International Tables for X-ray Crystallography*; Kynoch: Birmingham, England, 1965; Vol. 1. [b] Cell dimensions were determined by least-squares fit of the setting angles for 25 reflections with 2θ in the range 17–25 deg. [c] By the flotation method in ethanol/carbon tetrachloride. [d] The quantity minimized in the least-squares procedures is: $\sum w(|F_o| - |F_c|)^2$. $R_1 = \sum||F_o| - |F_c||/\sum|F_o|$. $R_2 = [\sum w(|F_o| - |F_c|)^2/\sum w(F_o)^2]^{1/2}$. [e] G. M. Sheldrick, SHELXTL, A Program For Crystal Structure Determination. Version 5.1. 1985. Nicolet Analytical Instruments, Madison, Wisconsin. [f] *International Tables for X-ray Crystallography*; Kynoch: Birmingham, England, 1974; Vol. 4.

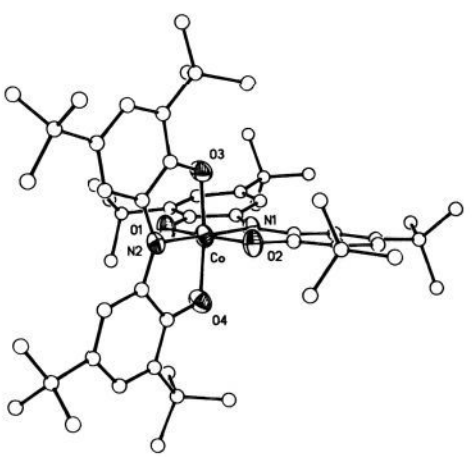

Figure 1. A plot showing the structure of the Co(Cat-N-BQ)(Cat-N-SQ) molecule. The manganese complex $Mn(Cat\text{-}N\text{-}SQ)_2$, is approximately isostructural with the differences in bond lengths and angles noted in the text and in the tables.

Co complex indicate that the Schiff base ligands occupy meridional sites of an octahedron, giving a complex molecule of approximate D_{2d} symmetry. A view of the molecule is given in Figure 1, and bond distances and angles are given in Table IV. The average Co–O length of 1.896 (5) Å and Co–N length of 1.868 (5) Å point to a specific charge for the metal ion. Bond lengths to Co(II) are typically 0.2 Å longer than bonds to oxygen and nitrogen donor

Table II. Atomic Coordinates (×10^4) and Isotropic Thermal Parameters (Å^2 × 10^3) for $Mn(C_{28}H_{40}NO_2)_2$

	x/a	y/b	z/c	U^a
Mn	4875 (1)	7327 (1)	2501 (1)	40 (1)
N1	*4923 (5)*	*7352 (4)*	*1594 (2)*	*39 (2)*
O1	3873 (4)	5854 (3)	2220 (2)	49 (2)
O2	5916 (4)	8795 (3)	2551 (2)	46 (2)
C1	3554 (6)	5619 (5)	1562 (3)	42 (3)
C2	2736 (6)	4599 (5)	1245 (3)	49 (3)
C3	2489 (6)	4507 (6)	557 (4)	56 (3)
C4	2999 (7)	5319 (6)	169 (3)	49 (3)
C5	3793 (6)	6290 (5)	483 (3)	48 (3)
C6	4112 (6)	6458 (5)	1187 (3)	41 (3)
C7	2208 (7)	3677 (5)	1667 (3)	61 (3)
C8	1276 (8)	2682 (6)	1221 (4)	93 (5)
C9	1525 (8)	4143 (7)	2114 (4)	83 (4)
C10	3300 (8)	3278 (6)	2097 (4)	85 (4)
C11	2601 (7)	5110 (6)	−590 (3)	69 (4)
C12	1262 (11)	5116 (13)	−863 (5)	204 (9)
C13	2788 (10)	4025 (7)	−801 (4)	109 (5)
C14	3429 (13)	5992 (9)	−916 (4)	181 (8)
C15	5722 (6)	8290 (5)	1440 (3)	36 (3)
C16	6053 (6)	8509 (5)	841 (3)	44 (3)
C17	6828 (6)	9511 (5)	781 (3)	42 (3)
C18	7285 (6)	10307 (5)	1336 (3)	47 (3)
C19	7011 (6)	10125 (5)	1939 (3)	40 (3)
C20	6236 (6)	9082 (5)	1993 (3)	38 (3)
C21	7221 (6)	9776 (5)	132 (3)	51 (3)
C22	8556 (7)	9669 (9)	234 (4)	106 (5)
C23	7154 (11)	10947 (7)	−61 (5)	117 (6)
C24	6355 (8)	8986 (8)	−461 (4)	105 (5)
C25	7496 (6)	11010 (5)	2527 (3)	49 (3)
C26	8383 (8)	12057 (6)	2371 (4)	83 (4)
C27	8209 (7)	10580 (6)	3155 (3)	66 (4)
C28	6354 (7)	11360 (6)	2666 (4)	78 (4)
N2	4828 (4)	7389 (4)	3416 (2)	39 (2)
O3	3443 (4)	7890 (3)	2371 (2)	45 (2)
O4	6272 (4)	6736 (3)	2856 (2)	48 (2)
C29	3176 (6)	8137 (5)	2923 (3)	41 (3)
C30	2198 (7)	8652 (5)	2916 (3)	47 (3)
C31	1998 (7)	8841 (5)	3528 (3)	54 (3)
C32	2707 (7)	8578 (6)	4145 (4)	56 (4)
C33	3656 (7)	8086 (5)	4136 (3)	52 (3)
C34	3911 (6)	7862 (5)	3527 (3)	42 (3)
C35	1429 (7)	8967 (6)	2263 (4)	64 (4)
C36	408 (9)	9500 (9)	2377 (5)	112 (6)
C37	799 (7)	7953 (7)	1786 (4)	91 (4)
C38	2305 (9)	9807 (7)	1962 (4)	95 (5)
C39	2413 (7)	8842 (6)	4818 (3)	74 (4)
C40	2561 (10)	10035 (9)	4895 (6)	102 (6)[b]
C40′	1092 (10)	9089 (8)	4693 (6)	101 (7)[b]
C41	1195 (9)	8189 (9)	4823 (7)	111 (6)[b]
C41′	2426 (9)	7789 (9)	5223 (6)	87 (6)[b]
C42	3333 (11)	8533 (8)	5399 (7)	127 (7)[b]
C42′	3337 (9)	9774 (9)	5191 (6)	104 (7)[b]
C43	*6492 (6)*	*6599 (5)*	*3504 (3)*	*42 (3)*
C44	5736 (6)	6990 (5)	3848 (3)	39 (3)
C45	5970 (7)	6909 (6)	4544 (3)	55 (3)
C46	6903 (7)	6448 (6)	4885 (4)	60 (4)
C47	7608 (7)	6043 (6)	4516 (4)	59 (4)
C48	7441 (6)	6100 (5)	3835 (3)	46 (3)
C49	7211 (7)	6358 (7)	5628 (3)	81 (4)
C50	7197 (9)	5145 (7)	5797 (4)	114 (5)
C51	6256 (10)	6680 (12)	5923 (4)	164 (8)
C52	8496 (8)	7102 (8)	5953 (4)	109 (5)
C53	8145 (7)	5557 (6)	3447 (4)	65 (4)
C54	9045 (8)	4972 (8)	3900 (4)	106 (5)
C55	8876 (8)	6433 (7)	3090 (4)	96 (5)
C56	7189 (8)	4660 (7)	2925 (4)	100 (5)

[a] Equivalent isotropic U defined as one-third of the trace of the orthogonalized U_{ij} tensor. [b] Atoms refined with occupancy factors of 0.5 and isotropic thermal parameters.

Table III. Atomic Coordinates ($\times 10^4$) and Isotropic Thermal Parameters ($Å^2 \times 10^3$) for $Co(C_{28}H_{40}NO_2)_2$

	x/a	y/b	z/c	U[a]
Co	4860 (1)	7327 (1)	2495 (1)	34 (1)
N1	4898 (4)	7322 (4)	1600 (2)	32 (2)
O1	3802 (4)	5870 (3)	2263 (2)	43 (2)
O2	5936 (4)	8784 (3)	2591 (2)	42 (2)
C1	3500 (6)	5637 (5)	1615 (3)	38 (3)
C2	2676 (6)	4602 (5)	1301 (3)	41 (3)
C3	2404 (6)	4471 (5)	612 (3)	49 (3)
C4	2898 (6)	5282 (5)	214 (3)	44 (3)
C5	3714 (6)	6244 (5)	515 (3)	43 (3)
C6	4069 (5)	6431 (4)	1221 (3)	36 (2)
C7	2146 (7)	3691 (5)	1724 (3)	55 (3)
C8	1208 (8)	2680 (6)	1278 (4)	86 (4)
C9	1439 (7)	4141 (6)	2170 (4)	72 (4)
C10	3247 (7)	3304 (6)	2148 (4)	75 (4)
C11	2478 (8)	5049 (6)	−543 (3)	67 (4)
C12	1036 (10)	4874 (10)	−788 (5)	167 (8)
C13	2776 (9)	4001 (7)	−749 (4)	100 (5)
C14	3072 (13)	5970 (7)	−899 (4)	228 (10)
C15	5697 (5)	8248 (4)	1460 (3)	32 (2)
C16	6018 (5)	8485 (5)	857 (3)	39 (3)
C17	6810 (6)	9476 (5)	798 (3)	39 (3)
C18	7278 (6)	10267 (5)	1352 (3)	42 (3)
C19	7013 (5)	10103 (4)	1966 (3)	34 (2)
C20	6216 (5)	9046 (5)	2033 (3)	35 (3)
C21	7189 (6)	9742 (5)	144 (3)	44 (3)
C22	8556 (7)	9688 (8)	246 (4)	97 (5)
C23	7071 (9)	10887 (7)	−48 (4)	101 (5)
C24	6358 (8)	8923 (7)	−442 (3)	95 (4)
C25	7479 (6)	10998 (5)	2543 (3)	45 (3)
C26	8373 (7)	12044 (5)	2392 (4)	73 (4)
C27	8229 (6)	10565 (6)	3176 (3)	65 (3)
C28	6335 (7)	11315 (6)	2684 (4)	67 (4)
N2	4812 (4)	7383 (4)	3387 (2)	34 (2)
O3	3452 (4)	7932 (3)	2330 (2)	41 (2)
O4	6262 (4)	6708 (3)	2793 (2)	44 (2)
C29	3182 (6)	8138 (5)	2882 (3)	37 (3)
C30	2200 (6)	8663 (5)	2892 (3)	44 (3)
C31	1981 (6)	8849 (5)	3502 (3)	47 (3)
C32	2656 (6)	8545 (5)	4115 (3)	48 (3)
C33	3586 (6)	8041 (5)	4105 (3)	47 (3)
C34	3887 (5)	7832 (5)	3493 (3)	36 (3)
C35	1464 (7)	9027 (6)	2237 (3)	59 (3)
C36	450 (7)	9588 (8)	2362 (4)	97 (5)
C37	811 (7)	8004 (7)	1738 (4)	85 (4)
C38	2385 (8)	9882 (6)	1956 (4)	83 (4)
C39	2348 (6)	8800 (5)	4780 (3)	68 (4)
C40	3318 (11)	8477 (10)	5388 (6)	60 (5)[b]
C40′	3520 (12)	9652 (9)	5245 (5)	66 (7)[b]
C41	2460 (11)	10062 (9)	4863 (5)	68 (6)[b]
C41′	1198 (11)	9297 (8)	4625 (7)	86 (9)[b]
C42	996 (12)	8122 (9)	4769 (6)	83 (7)[b]
C42′	2743 (11)	7773 (10)	5302 (6)	93 (9)[b]
C43	6479 (6)	6599 (5)	3437 (3)	38 (3)
C44	5739 (5)	7001 (4)	3795 (3)	34 (2)
C45	6002 (6)	6934 (5)	4497 (3)	48 (3)
C46	6929 (6)	6462 (6)	4821 (3)	54 (3)
C47	7619 (6)	6039 (5)	4440 (3)	54 (3)
C48	7414 (6)	6073 (5)	3770 (3)	43 (3)
C49	7249 (7)	6375 (7)	5576 (3)	68 (3)
C50	7193 (8)	5151 (7)	5725 (4)	106 (5)
C51	6354 (9)	6761 (10)	5894 (4)	140 (7)
C52	8575 (7)	7075 (7)	5892 (4)	96 (4)
C53	8129 (7)	5523 (6)	3371 (4)	60 (3)
C54	9058 (8)	4957 (7)	3816 (4)	93 (5)
C55	8870 (7)	6392 (7)	3005 (4)	86 (4)
C56	7169 (8)	4626 (6)	2854 (4)	87 (4)

[a] Equivalent isotropic U defined as one-third of the trace of the orthogonalized U_{ij} tensor. [b] Atoms refined with occupancy factors of 0.5 and isotropic thermal parameters.

ligands coordinated to Co(III). These values are well within the range of Co(III) values. For comparison, Co–O and C–O lengths of the Co(III) complex containing mixed-charge quinone ligands Co^{III}(bpy)(DBSQ)(DBCat) average to 1.883 (6) and 1.949 (7) Å,[9] while Co^{II}–O lengths of the Co^{II}_4(DBSQ)$_8$ tetramer range from 2.045 (3) to 2.225 (3) Å.[13] As a complex of Co(III), the two biquinone ligands are required to be of different charge, Co(Cat-N-BQ)(Cat-N-SQ). Even though they are crystallographically nonequivalent, both ligands have similar structural features, suggesting charge delocalization over the entire molecule. The C–O and C–N lengths do not differ significantly and average to 1.305 (7) and 1.362 (7) Å. Bond lengths within the two ligands show evidence of delocalization and the planes about the two nitrogen atoms defined by the two phenyl carbon atoms and the Co show no significant deviations from planarity. The two ligands differ in the degree of planarity of the phenyl rings, however. There is a 0.7° twist between phenyl ring planes of the ligand containing O3, N2, O4, while the twist angle between rings of the ligand containing O1, N1, O2 is 13.1°. This appears to result from packing in the crystal structure.

Table IV. Selected Bond Distances and Angles for $Co(C_{28}H_{40}NO_2)_2$

Distances (Å)			
Co–N1	1.869 (5)	Co–N2	1.868 (5)
Co–O1	1.896 (3)	Co–O3	1.885 (5)
Co–O2	1.900 (3)	Co–O4	1.904 (5)
O1–C1	1.313 (7)	O3–C29	1.295 (8)
O2–C20	1.300 (7)	O4–C43	1.313 (7)
N1–C6	1.355 (6)	N2–C34	1.364 (9)
N1–C15	1.367 (7)	N2–C44	1.363 (7)
C1–C6	1.428 (8)	C29–C34	1.430 (8)
C1–C2	1.431 (7)	C29–C30	1.426 (10)
C2–C3	1.385 (9)	C30–C31	1.378 (10)
C3–C4	1.413 (9)	C31–C32	1.420 (9)
C4–C5	1.354 (8)	C32–C33	1.357 (11)
C5–C6	1.419 (8)	C33–C34	1.431 (10)
C15–C20	1.445 (7)	C43–C44	1.420 (10)
C15–C16	1.404 (9)	C44–C45	1.420 (8)
C16–C17	1.365 (8)	C45–C46	1.364 (10)
C17–C18	1.410 (8)	C46–C47	1.420 (11)
C18–C19	1.387 (9)	C47–C48	1.355 (9)
C19–C20	1.434 (7)	C43–C48	1.420 (9)
Angles (deg)			
O1–Co–O2	171.3 (2)	Co–O1–C1	110.4 (3)
O1–Co–N1	85.5 (2)	Co–O2–C20	110.8 (3)
O2–Co–N1	85.7 (2)	Co–O3–C29	110.7 (4)
O3–Co–O4	171.6 (2)	Co–O4–C43	110.3 (4)
O3–Co–N2	85.8 (2)	Co–N1–C6	112.9 (4)
O4–Co–N2	85.8 (2)	Co–N1–C15	113.4 (3)
O1–Co–O3	91.2 (2)	Co–N2–C34	113.2 (4)
O1–Co–O4	89.0 (2)	Co–N2–C44	112.9 (4)
O2–Co–O3	89.6 (2)	O1–C1–C6	118.1 (4)
O2–Co–O4	91.5 (2)	O2–C20–C15	118.8 (5)
N1–Co–N2	177.9 (2)	O3–C29–C34	119.2 (6)
O1–Co–N2	95.9 (2)	O4–C43–C44	118.6 (5)
O2–Co–N2	92.8 (2)	N1–C6–C1	112.0 (5)
O3–Co–N1	92.7 (2)	N1–C15–C20	110.9 (5)
O4–Co–N1	95.7 (2)	N2–C34–C29	111.0 (5)
C6–N1–C15	133.5 (5)	N2–C44–C43	112.2 (5)
C34–N2–C44	133.8 (5)		

Crystallographic Structure Determination on Mn(Cat-N-SQ)$_2$. The crystal and molecular structures of the manganese complex are identical with those of the cobalt complex. Since bond distances and angles provide information on charge distribution, a full independent structure determination was carried out. Lengths and angles obtained for the complex molecule are given in Table V. The octahedron is quite regular with Mn–O and Mn–N lengths which average to 1.896 (5) and 1.910 (5) Å, respectively. These values are significantly shorter than values expected for Mn(II), but they are within the range of lengths found for complexes of Mn(IV). *trans*-Mn(py)$_2$(DBCat)$_2$ was reported to have Mn–O and Mn–N lengths of 1.854 (2) and 2.018 (3) Å,[5] and the bis(salicylate) complex Mn(bpy)(Sal)$_2$ was observed to have values of 1.852 (5) and 2.046 (6) Å.[14] While, in the present case, Mn–O lengths are slightly longer and Mn–N lengths slightly shorter than

(13) Buchanan, R. M.; Fitzgerald, B. J.; Pierpont, C. G. *Inorg. Chem.* **1979**, *18*, 3439.
(14) Pavacik, P. S.; Huffman, J. C.; Christou, G. *J. Chem. Soc., Chem. Commun.* **1986**, 43.

Table V. Selected Bond Distances and Angles for $Mn(C_{28}H_{40}NO_2)_2$

	Distances (Å)		
Mn–N1	1.901 (6)	Mn–N2	1.918 (6)
Mn–O1	1.901 (5)	Mn–O3	1.886 (6)
Mn–O2	1.901 (5)	Mn–O4	1.894 (6)
O1–C1	1.332 (7)	O3–C29	1.313 (10)
O2–C20	1.330 (8)	O4–C43	1.325 (8)
N1–C6	1.374 (7)	N2–C34	1.382 (10)
N1–C15	1.388 (8)	N2–C44	1.378 (8)
C1–C6	1.427 (9)	C29–C34	1.414 (9)
C1–C2	1.417 (8)	C29–C30	1.410 (11)
C2–C3	1.383 (10)	C30–C31	1.378 (11)
C3–C4	1.403 (10)	C31–C32	1.414 (10)
C4–C5	1.362 (9)	C32–C33	1.370 (13)
C5–C6	1.416 (9)	C33–C34	1.411 (11)
C15–C20	1.411 (8)	C43–C44	1.417 (11)
C15–C16	1.400 (10)	C44–C45	1.411 (9)
C16–C17	1.366 (9)	C45–C46	1.369 (11)
C17–C18	1.417 (9)	C46–C47	1.413 (13)
C18–C19	1.375 (10)	C47–C48	1.382 (11)
C19–C20	1.400 (9)	C43–C48	1.404 (10)
	Angles (deg)		
O1–Mn–O2	165.1 (2)	Mn–O1–C1	114.1 (4)
O1–Mn–N1	82.8 (2)	Mn–O2–C20	114.5 (3)
O2–Mn–N1	82.4 (2)	Mn–O3–C29	114.6 (4)
O3–Mn–O4	165.4 (2)	Mn–O4–C43	114.4 (5)
O3–Mn–N2	82.7 (2)	Mn–N1–C6	114.6 (4)
O4–Mn–N2	82.7 (2)	Mn–N1–C15	115.2 (4)
O1–Mn–O3	91.6 (2)	Mn–N2–C34	114.0 (4)
O1–Mn–O4	89.3 (2)	Mn–N2–C44	114.6 (5)
O2–Mn–O3	90.8 (2)	O1–C1–C6	115.7 (5)
O2–Mn–O4	92.0 (2)	O2–C20–C15	116.6 (5)
N1–Mn–N2	176.8 (2)	O3–C29–C34	117.1 (7)
O1–Mn–N2	99.9 (2)	O4–C43–C44	116.9 (6)
O2–Mn–N2	95.0 (2)	N1–C6–C1	111.6 (5)
O3–Mn–N1	95.4 (2)	N1–C15–C20	110.9 (5)
O4–Mn–N1	99.2 (2)	N2–C34–C29	111.2 (6)
C6–N1–C15	130.1 (5)	N2–C44–C43	111.3 (5)
C34–N2–C44	131.4 (5)		

values found in other complexes, the metal appears to be Mn(IV). The biquinone ligands in this charge formulation are in the radical dianionic Cat-N-SQ electronic form $Mn(Cat\text{-}N\text{-}SQ)_2$. In accord with this, average C–O and C–N lengths of 1.325 (8) and 1.381 (8) Å are 0.02 Å longer than values found for the Co complex, reflecting an increased order of reduction. As before, the nitrogens are planar and the ligand containing O1, N1, O2 shows a twist of 13.4° between phenyl rings while the other ligand is more rigorously planar.

The pattern of carbon–carbon bond lengths for the eight phenyl rings of the four ligands of both structure determinations shows values that point to an unusually *localized* electronic structure. In all eight rings the bonds between carbon atoms at the 3 and 4 ring positions, and between carbon atoms 5 and 6, are consistently shorter than the other four bonds. Values at these two positions average to 1.372 (4) Å for the Mn complex and 1.368 (5) Å for the Co molecule, while other C–C bond values in the rings are 1.40 Å or greater. Charge delocalization within the ligand appears to be contained primarily within the region of the C–O and C–N bonds.

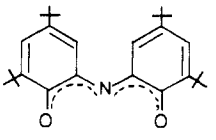

Magnetism and EPR on $Mn(Cat\text{-}N\text{-}SQ)_2$ and Co(Cat-N-BQ)(Cat-N-SQ). In studies on complexes consisting of paramagnetic metal ions chelated by semiquinone ligands, spin–spin coupling between unpaired electrons on ligand and metal is generally observed.[6,15] The d^3 Mn(IV) ion of $Mn(Cat\text{-}N\text{-}SQ)_2$ is strongly coupled to the two $S = {}^1/_2$ radical ligands to give a complex with one unpaired electron. The magnetic moment of the complex is 1.79 μ_B, and the EPR signal of the complex in pentane solution at room temperature consists of six lines centered about a $\langle g \rangle$ value of 2.013. The six-line spectrum arises from coupling of 104 G to the $I = {}^5/_2$ ^{55}Mn nucleus. Each of the six lines is further split into 5 lines, as shown in Figure 2, by the two equivalent $I = 1$ ^{14}N nucleii. A rhombic anisotropic spectrum is observed for the complex in a toluene/chloroform glass at −196 °C with $g_\parallel$ and $g_\perp$ of 1.977 and 2.040 and $A_\parallel$ and $A_\perp$ values of 153 and 84.2 G to the ^{55}Mn nucleus.

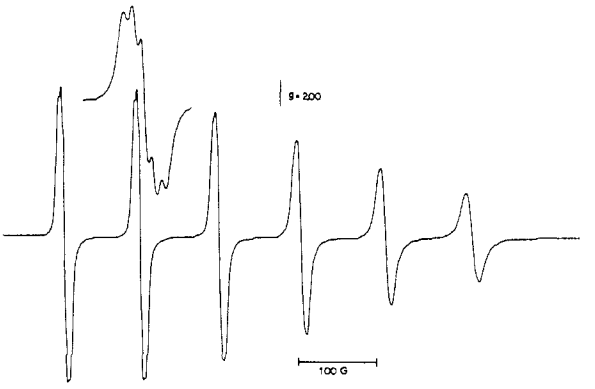

Figure 2. Isotropic EPR spectrum of $Mn(Cat\text{-}N\text{-}SQ)_2$ recorded in toluene solution. The spectrum is centered about a $\langle g \rangle$ value of 2.013 and shows ^{55}Mn hyperfine coupling of 104 G and ^{14}N coupling of 3.8 G to two equivalent nucleii. An insert showing the nitrogen hyperfine on one line is included.

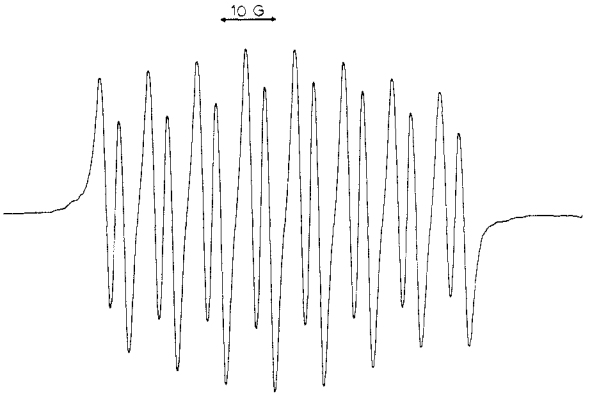

Figure 3. Isotropic EPR spectrum of Co(Cat-N-BQ)(Cat-N-SQ) recorded in pentane and in toluene solutions. The spectrum remains unchanged over temperatures ranging from −100 to +80 °C.

The cobalt complex, Co(Cat-N-BQ)(Cat-N-SQ) with mixed charge ligands, also contains a single unpaired electron, but in this case spin density is concentrated on the radical ligands. The magnetic moment of the complex was determined to be 1.89 μ_β at room temperature, and the EPR signal of the complex is shown in Figure 3. The magnetic moment is slightly higher than the expected spin-only value for a $S = {}^1/_2$ molecule, but it compares well with the room temperature value of 1.92 μ_β measured for Co(bpy)(DBSQ)(DBCat) which is also a radical-centered spin system coordinated to diamagnetic Co(III).[9] The EPR spectrum is centered about a $\langle g \rangle$ value of 1.9974 and consists of 16 lines. The spectrum appears to arise from coupling of 9.3 G to the $I = {}^7/_2$ ^{59}Co nucleus with each line split by coupling of 3.4 G to a single $I = {}^1/_2$ nucleus, presumably one proton. This spectrum closely resembles the spectrum of Co(salen)(DBSQ) which shows cobalt coupling of 10.2 G and coupling to a single ring proton of 3.5 G.[16] Even upon high resolution the spectrum of Co(Cat-N-BQ)(Cat-N-SQ) fails to show the expected nitrogen hyperfine, nor does it show the more complicated proton coupling pattern of the delocalized radical.[12] A pentane solution of the complex

(15) Lynch, M. W.; Buchanan, R. M.; Pierpont, C. G.; Hendrickson, D. N. *Inorg. Chem.* **1981**, *20*, 1038.

(16) Kessel, S. L.; Emberson, R. M.; Debrunner, P. G.; Hendrickson, D. N. *Inorg. Chem.* **1980**, *19*, 1170.

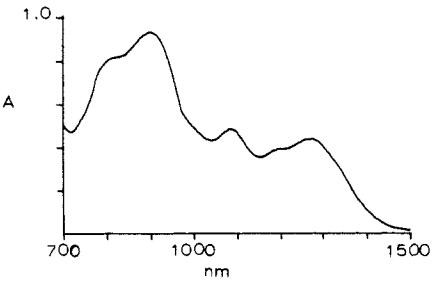

Figure 4. The visible and near-infrared spectrum of $Mn(Cat\text{-}N\text{-}SQ)_2$ recorded in toluene solution at room temperature.

was cooled to −100 °C with loss of hyperfine, but with no changes in the general appearance of the spectrum or in hyperfine coupling constants. This suprising result points to an electronic structure for the complex which, on the ERP time scale, contains a single unpaired electron localized in one region of one ligand of the complex molecule and coupled to only one ligand proton.

Spectral Properties of $Mn(Cat\text{-}N\text{-}SQ)_2$ and Co(Cat-N-BQ)(Cat-N-SQ). Infrared spectra on the Co and Mn complexes were compared with spectra obtained on the Zn and Fe analogues reported by Girgis and Balch.[10] The zinc complex is a clear example of Cat-N-BQ coordination to Zn(II) and should serve as a spectroscopic benchmark for ligand coordination in that electronic form. Mössbauer spectra on the iron complex indicate high-spin Fe(III),[17] and this complex is similar in form to the cobalt molecule with mixed charge ligands.

Spectra obtained on all four complexes show similar features in the region between 700 and 1200 cm^{-1} which are relatively insensitive to ligand charge. A strong band which appears at approximately 1000 cm^{-1} for the Zn, Co, and Fe complexes is increased to 1050 cm^{-1} for $Mn(Cat\text{-}N\text{-}SQ)_2$ and strong bands at 1200 cm^{-1} for the Co and Zn complexes are shifted to 1170 cm^{-1} for the Fe complex and to 1162 for the Mn complex. The region from 1200 to 1600 cm^{-1} should contain the C–O and C–N stretching vibrations mixed with ring vibrational modes and be most sensitive to charge distribution in the complex. The Mn complex shows three prominent peaks at 1231, 1315, and 1362 cm^{-1} and a less intense envelope of peaks between 1400 and 1500 cm^{-1}. The intensity and position of bands observed for the Fe and Co complexes are nearly identical with the exception of a strong band at 1520 cm^{-1} which is present in the Fe spectrum but absent in the Co spectrum. Otherwise, the 1200 to 1600 cm^{-1} region of the Co spectrum is similar to the Mn spectrum with an additional intense band at 1285 cm^{-1}. The Zn complex shows a very strong absorption at this position and it is tempting to describe the Co and Fe spectra as a superposition of the Zn and Mn spectra. To a rough approximation this is true; however, shifts in band position and intensity differences prevent the correlation from being exact.

The complexes of the Cat-N-BQ ligand are highly colored due to intense absorptions in the visible region of the spectrum. The Zn complex $Zn(Cat\text{-}N\text{-}BQ)_2$ is dark green in color due to two transitions in the 750-nm region with molar extinction coefficients near 40 000. With Co and Mn, and a difference in charge distribution, the electronic spectra extend out to low energy into the near-infrared. In toluene solution, Co(Cat-N-BQ)(Cat-N-SQ) shows bands at 388 (12 800 L mol^{-1} cm^{-1}), 436 (8 900), 532 (9 100), and 794 (8 300) nm. The spectrum extends into the near-IR with a shoulder on the 794-nm band at 890 and an additional band at 1030 (5 300) nm. The spectrum of $Mn(Cat\text{-}N\text{-}SQ)_2$ shown in Figure 4 extends even further into the near-IR. Higher energy bands appear at 346 (22 000), 476 (11 200), and 856 (10 000) nm. Four transitions are observed in the near-IR at 900 (9 300), 1087 (4 000), 1200 (sh), and 1268 (4 300) nm. From the charge distribution within the complex it seems reasonable to assign these as ligand-to-metal charge-transfer transitions which arise from metal and ligand localized electronic levels which are quite close in energy.

Electrochemistry on Co(Cat-N-BQ)(Cat-N-SQ) and $Mn(Cat\text{-}N\text{-}SQ)_2$. Both the metals and ligands of these complexes may show electrochemical activity. The cobalt complex undergoes one-electron oxidation and reduction reversibly in dichloromethane solutions. Oxidation occurs at −0.315 V (ΔE = 68 mV), relative to the ferrocenium/ferrocene couple, and probably involves oxidation of the more reduced ligand to give the Co(III) cation $Co(Cat\text{-}N\text{-}BQ)_2^+$. Reduction occurs at −0.897 V (ΔE = 68 mV) and, from the reversibility of the couple, it also appears to occur at a ligand to give $Co(Cat\text{-}N\text{-}SQ)_2^-$. At a more negative potential the complex undergoes a second quasireversible one-electron reduction, −1.716 V (ΔE = 164 mV). This process probably occurs at the metal to give the Co(II) complex $Co(Cat\text{-}N\text{-}SQ)_2^{2-}$.

The manganese complex also undergoes a one-electron oxidation and two one-electron reductions, but all three processes are reversible at a scan rate of 50 mV/s in dichloromethane. Oxidation occurs at +0.208 (ΔE = 67 mV) and, as before, it appears to involve one of the ligands to give the mixed-charge ligand complex $Mn(Cat\text{-}N\text{-}BQ)(Cat\text{-}N\text{-}SQ)^+$. The two reductions at −0.945 V (ΔE = 70 mV) and −1.484 V (ΔE = 67 mV) both probably occur at the metal to give Mn(III) and Mn(II) complexes with the ligand remaining in the Cat-N-SQ form.

Discussion

Many of the features which have made the coordination chemistry of the semiquinonate and catecholate ligands of great interest appear to be carried over to the Schiff base biquinone ligands included in this investigation. Antiferromagnetic coupling between radical semiquinonates and paramagnetic metal ions is commonly observed for the quinone complexes, and a similar interaction is responsible for the $S = {}^1/_2$ ground state of $Mn(Cat\text{-}N\text{-}SQ)_2$. The ability of catecholate ligands to stabilize high oxidation state metal ions, including Mn(IV), is a property which also appears common to the biquinone ligand. The EPR spectrum of the mixed-charge ligand complex of cobalt, Co(Cat-N-BQ)(Cat-N-SQ), shows that the electronic structure of ligand and metal remain discrete. The spectrum is surprising in that it shows weak coupling to the metal and to only one additional ring proton. Bond distances within the phenyl rings of the ligands show evidence of charge localization. However, the spectrum suggests an even more localized electronic structure for the radical ligand, one with the unpaired spin trapped on a single carbon center on the EPR time scale. EPR studies on the protonated form of the radical[12] and on the tin complex $SnPh_2(Cat\text{-}N\text{-}SQ)$ have appeared.[18] Both show coupling to the nitrogen and to sets of equivalent protons at the 3 and 5 ring positions. Spectra of both species are more complicated than the simple 16 line spectrum of Co(Cat-N-BQ)(Cat-N-SQ), and the spectrum of the cobalt complex appears to reflect an intrinsic electronic property of the molecule.

Acknowledgment. This research was supported by the National Science Foundation under Grants CHE 85-03222 and CHE 84-12182 (X-ray instrumentation).

Registry No. $Co(C_{28}H_{40}NO_2)_2$, 112506-13-5; $Mn(C_{28}H_{40}NO_2)_2$, 112506-14-6; 3,5-di-*tert*-butylcatechol, 1020-31-1; ammonia, 7664-41-7.

Supplementary Material Available: Tables containing anisotropic thermal parameters, bond distances, and angles for $Mn(C_{28}H_{40}NO_2)_2$ and $Co(C_{28}H_{40}NO_2)_2$ (5 pages); listing of observed and calculated structure factors (43 pages). Ordering information is given on any current masthead page.

(17) The neutral iron complex Fe(Cat-N-BQ)(Cat-N-SQ)[10] has a magnetic moment of 5.33 μ_B due to coupling between the radical ligand and the high-spin metal center.

(18) Stegmann, H. B.; Scheffler, K. *Chem. Ber.* **1970**, *103*, 1279.